First-principles study of solute diffusion in Ni_3Al*

Shaohua Liu(刘少华)[1], Zi Li(李孜)[2], and Chongyu Wang(王崇愚)[3,†]

[1] School of Materials Science and Engineering, Tsinghua University, Beijing 100084, China
[2] Institute of Applied Physics and Computational Mathematics, Beijing 100088, China
[3] Department of Physics, Tsinghua University, Beijing 100084, China

(Received 3 June 2017; published online 18 July 2017)

Using first-principles calculations in combination with Wagner–Schottky and kinetic Monte Carlo methods, the diffusion behaviors of solutes via various vacancy-mediated diffusion mechanisms in $L1_2$ γ'-Ni_3Al were investigated. The formation energies of the point defects and the migration energies for solutes were calculated. Adding alloying elements can decrease the defect-formation energies of Ni_{Al}, increase the defect-formation energies of Al_{Ni}, and have little effect on the formation energy of V_{Ni}. The migration energies of solutes are related with the site preference and the diffusion mechanism. The diffusion coefficients of Ni, Al, and solutes were calculated, and the concentration of antisite defects plays a crucial role in the elemental diffusion.

Keywords: nickel-based superalloy, diffusion, Ni_3Al, first-principles

PACS: 31.15.A–, 71.15.Mb, 71.20, 66.30.–h **DOI:** 10.1088/1674-1056/26/9/093102

1. Introduction

γ'-Ni_3Al ($L1_2$ structure) intermetallic compounds as the key strengthening precipitates of nickel-based single-crystal superalloys play a decisive role in the excellent mechanical properties for blade applications in jet engines and land-based gas turbines.[1,2] In addition, $L1_2$ structure intermetallics have attracted a great deal of attention in recent years in connection with enormous potential structural materials for high-temperature applications due to their anomalous temperature dependence of the yield stress.[3,4] To improve the mechanical properties and temperature resistance of γ'-Ni_3Al, alloying elements, such as Ta, W, Re, Mo, and Cr, are often added.[5–7] In the investigation of creep and oxidation behavior at elevated temperature, diffusion plays an important role in the microstructure evolution,[8] planar deformation mechanisms,[9] and dislocation motion[10,11] for γ' precipitates.

Presently, there exist a large number of experimental works on self-diffusion and solute diffusion in model Ni_3Al intermetallic compound measured in a wide temperature range.[12–21] Some of these data sets were studied using tracer techniques.[12–14] Unfortunately, direct experimental measurements on the Al self-diffusion in Ni_3Al suffer from the lack of a suitable radiotracer Al. Thus, interdiffusion coefficients were measured using diffusion couples.[19,22,23] Due to the different concentrations of thermal defects (vacancies and anti-structure atoms) and sophisticated diffusion mechanisms in ordered intermetallics, the available data on the solute diffusion show a marked deviation and are often incomplete in the case of diffusion for alloying elements in ternary alloys. Therefore, a systematically theoretical investigation on the diffusion of alloying elements in ordered intermetallic compounds is important, not only from the fundamental scientific standpoint for gaining a deeper insight into the microscopic diffusion mechanisms, but also with the purpose of practical aspects for designing superior Ni-based superalloys.

In this work, we employed density functional theory (DFT) calculations to study the formation energy of point defects and migration barriers of ternary additions (Ti, Nb, Ta, Cr, Co, Mo, W, Re, Ru) in Ni_3Al. In addition, several potential diffusion mechanisms were also taken into account and the diffusivity of Ni, Al, and solutes was predicted by using kinetic Monte Carlo (KMC) simulations. This also provides the knowledge for the diffusion behavior of alloying elements in other $L1_2$ structure intermetallics (e.g., $Co_3(Al,W)$).

2. Computational methodology

Density-functional theory implementing in the Vienna *ab-initio* simulation package (VASP)[24] was used to investigate the vacancy formation and migration energies. All calculations were performed using the projector augmented-wave method[25,26] and the generalized gradient approximation in the Perdew–Burke–Ernzerhof form (GGA-PBE).[27] The minimum plane wave energy cutoff was 350 eV. A first-order Methfessel–Paxton smearing method[28] was used with a smearing width of SIGMA = 0.2 eV. The convergence accuracy of the total energies of electronic self-consistency was 10^{-5} eV. The Brillouin zone integration was performed with a $5 \times 5 \times 5$ Monkhorst–Pack[29] k-point scheme. Full

*Project supported by Beijing Municipality Science and Technology Commission, China (Grant No. D161100002416001) and the National Key R&D Program of China (Grant No. 2017YFB0701502).

†Corresponding author. E-mail: cywang@mail.tsinghua.edu.cn

© 2017 Chinese Physical Society and IOP Publishing Ltd

ionic relaxation was performed until the maximum Hellmann–Feynman force was lower than 0.02 eV/Å. The vacancy formation and migration energies in the Ni–Al–M ternary systems were calculated in a $3\times3\times3$ (108 lattice sites) $L1_2$-Ni_3Al supercell.

In the metal crystals, the dominant mechanism for the diffusion of matrix atoms and substitutional solutes is the vacancy mechanism.[30] Each atom moving through the crystal by this mechanism should satisfy two requirements: (i) a vacancy must exist at the first neighbor of the jumping atom, (ii) the thermal activation is sufficient to make an adjacent atom exchange with a vacancy. The exchange jump rate of atoms jumping into a particular neighboring site with the vacancy mechanism can be expressed as[30]

$$\Gamma = z\varpi C_{\mathrm{Va}}^{\mathrm{eq}}, \tag{1}$$

where ω denotes the jump rate between an atom and a vacancy, $C_{\mathrm{Va}}^{\mathrm{eq}}$ is the thermal equilibrium concentration of monovacancy in the crystal, and z is the coordination number.

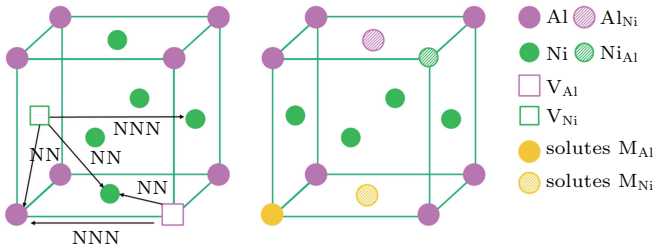


Fig. 1. (color online) Atomic configuration for ordered $L1_2$ Ni_3Al, with possible directions of the vacancy jumps and possible types of point defects. Ni atoms occupy the face-centered sites and Al atoms locate at the corner position. The arrows show nearest-neighbor (NN) and next-nearest-neighbor (NNN) vacancy jumps.

In the $L1_2$-Ni_3Al ordered structure as illustrated in Fig. 1, each Ni atom is surrounded by eight nearest neighbor (NN) Ni atoms and four Al atoms, while each Al atom is surrounded by 12 Ni atoms. There are four types of point defects that can form in Ni_3Al: V_{Ni} on the Ni sublattices, V_{Al} on the Al sublattices, Al_{Ni} antisite (anti-structure) atoms, and Ni_{Al} antisite atoms. The vacancy formation energies for Ni and Al atoms in the Ni_3Al (γ' phase) were calculated using the Wagner–Schottky model [31,32] as follows:

$$E_{\mathrm{V_{Ni}}}^{\mathrm{f}} = E_{\mathrm{Ni80Al27Va}} - E_{\mathrm{Ni81Al27}} + E_{\mathrm{Ni}}, \tag{2a}$$

$$E_{\mathrm{V_{Al}}}^{\mathrm{f}} = E_{\mathrm{Ni81Al26Va}} - E_{\mathrm{Ni81Al27}} + E_{\mathrm{Al}}, \tag{2b}$$

where $E_{\mathrm{Ni80Al27Va}}$, $E_{\mathrm{Ni81Al26Va}}$, and E_{Ni81Al27} are the energies of the supercells that contain one Ni vacancy, one Al vacancy, and no vacancy, respectively. E_{Ni} and E_{Al} are the total energies per atom in perfect Ni and Al fcc crystals, respectively. In the presence of solute M at the Al sublattice or Ni sublattice for a dilute substitutional Ni_3Al intermetallic with a vacancy, we have the expression

$$E_{\mathrm{V_{Ni}}}^{\mathrm{f}}(M_{\mathrm{Al}}) = E_{\mathrm{Ni80Al26}M\mathrm{Va}} - E_{\mathrm{Ni81Al26}M} + E_{\mathrm{Ni}}, \tag{3a}$$

$$E_{\mathrm{V_{Al}}}^{\mathrm{f}}(M_{\mathrm{Al}}) = E_{\mathrm{Ni81Al25}M\mathrm{Va}} - E_{\mathrm{Ni81Al26}M} + E_{\mathrm{Al}}, \tag{3b}$$

$$E_{\mathrm{V_{Ni}}}^{\mathrm{f}}(M_{\mathrm{Ni}}) = E_{\mathrm{Ni79}M\mathrm{Al27Va}} - E_{\mathrm{Ni80}M\mathrm{Al27}} + E_{\mathrm{Ni}}, \tag{3c}$$

$$E_{\mathrm{V_{Al}}}^{\mathrm{f}}(M_{\mathrm{Ni}}) = E_{\mathrm{Ni80}M\mathrm{Al26Va}} - E_{\mathrm{Ni80}M\mathrm{Al27}} + E_{\mathrm{Al}}. \tag{3d}$$

Based on the mean-field approximation and the mass-balance constraints, a set of non-linear equations can be determined through the minimization of the Gibbs free energy of the system ($\Delta G = \Delta H - T\Delta S = \min$). Then, the equilibrium concentrations of point defects can be obtained by solving the following set of non-linear equations:[32]

$$\frac{4x_{\mathrm{V_{Al}}}x_{\mathrm{Al_{Ni}}}}{x_{\mathrm{V_{Ni}}}\left(1-4x_{\mathrm{Ni_{Al}}}-3x_{\mathrm{V_{Al}}}+x_{\mathrm{V_{Ni}}}\right)} = \exp\left(-\frac{H_{\mathrm{Al_{Ni}}}-H_{\mathrm{V_{Ni}}}+H_{\mathrm{V_{Al}}}}{k_{\mathrm{B}}T}\right), \tag{4a}$$

$$\frac{4x_{\mathrm{V_{Ni}}}x_{\mathrm{Ni_{Al}}}}{x_{\mathrm{V_{Al}}}\left(3-4x_{\mathrm{Al_{Ni}}}+3x_{\mathrm{V_{Al}}}-x_{\mathrm{V_{Ni}}}\right)} = \exp\left(-\frac{H_{\mathrm{Ni_{Al}}}+H_{\mathrm{V_{Ni}}}-H_{\mathrm{V_{Al}}}}{k_{\mathrm{B}}T}\right), \tag{4b}$$

$$\frac{256x_{\mathrm{V_{Al}}}x_{\mathrm{V_{Ni}}}^3}{27\left(1+x_{\mathrm{V_{Al}}}+x_{\mathrm{V_{Ni}}}\right)^4} = \exp\left(-\frac{H_{\mathrm{V_{Al}}}+3H_{\mathrm{V_{Ni}}}}{k_{\mathrm{B}}T}\right), \tag{4c}$$

$$x_{\mathrm{Ni_{Al}}} - x_{\mathrm{Al_{Ni}}} + \frac{3+3x_{\mathrm{V_{Al}}}-x_{\mathrm{V_{Ni}}}}{4} = x_{\mathrm{Ni}}, \tag{4d}$$

where x_i and H_i denote the mole fraction and formation enthalpy of point defect i, respectively. Note that, all calculations are performed at approximately zero pressure, the enthalpy H_i is equal to the energy E_i. x_{Ni} is the total mole fraction of Ni in the alloy. For the stoichiometric $L1_2$ Ni_3Al, $x_{\mathrm{Ni}} = 0.75$. For a given composition and temperature, the equilibrium concentrations of all point defects can be obtained by solving Eq. (4).

Based on the harmonic transition state theory (hTST),[33–36] the jump rate can be expressed as

$$\omega = \nu^0 \exp\left(-\frac{E^{\mathrm{m}}}{k_{\mathrm{B}}T}\right), \tag{5}$$

where ω is the number of jumps per unit time to a neighboring site and ν^0 is the attempt frequency, which is of the order of the Debye frequency $\nu_0 = 10^{13}$ Hz. E^{m} is the migration barrier of Al, Ni, and M solutes, which is calculated using the climbing image nudged elastic band method (CI-NEB) as implemented in the VTST package[37] for VASP. Three image CI-NEB calculations were used to determine the minimum energy path. Then, the images were fully relaxed until the total energy of electronic self-consistency was below 10^{-5} eV and the maximum Hellmann–Feynman force was below 0.02 eV/Å.

According to the Einstein–Smoluchowski (ES) relation,[30] the coefficient of diffusion is directly related with the mean square displacement of atoms and can be written as

$$D = \frac{\langle L^2 \rangle}{6\tau}, \tag{6}$$

where $\langle L^2 \rangle$ is the total mean square displacement and τ is the simulation time in the simulation with averages taken over 10^5 KMC trajectories. In each trajectory, 10^5 transitions are considered.

As mentioned above, the fractions of the Al and the Al-substituting solutes on the Ni sublattice should be considered. Then, the exchange jump rate can be obtained as

$$\Gamma = z\varpi C_{\mathrm{Va}}^{\mathrm{eq}} p_M, \tag{7}$$

where p_M denotes the fraction of elements on Ni sublattice. By neglecting the concentration of the Al vacancy concentration, $p_{\mathrm{Al}} \cong 4x_{\mathrm{Al_{Ni}}}$ can be written for the stoichiometric composition.

Introducing the exchange jump rate Γ into Eq. (6), we then have

$$D = \frac{\langle d^2 z \Gamma \rangle}{6}, \tag{8}$$

where d is the jump length, with a value of $a\sqrt{2}/2$ for the fcc Bravais lattices.

The concentrations of point defects and the jump rate were included in the kinetic Monte Carlo (KMC) model[34,38] to calculate the diffusion rate at any particular temperature. Details of the KMC simulations can be found in our previous publication.[36]

3. Results and discussion

3.1. Concentration of point defects

The point-defect formation energies E_{defect} are listed in Table 1. The formation energy of $\mathrm{Al_{Ni}}$ is < 0 eV, indicating that it is favorable for the defect to form. The vacancy formation energies are higher than the antisite formation energies, which agrees with earlier results in the literature.[32,39] In the Ni–Al binary phase diagram, a narrow composition interval exists on both sides of the stoichiometric compositions, which are accommodated by antisite atoms ($\mathrm{Al_{Ni}}$ and $\mathrm{Ni_{Al}}$). By numerically solving Eq. (4) with the point-defects formation energies given in Table 1, the concentrations of point defects in stoichiometric $\mathrm{Ni_3Al}$ as a function of temperature are shown in Fig. 2. Through a linear fit to the relationship

$$\tilde{E}_{\mathrm{defect}} = -k_{\mathrm{B}} \frac{\partial \ln x_{\mathrm{defect}}}{\partial (1/T)},$$

the effective defect formation energies are obtained from Fig. 2 and listed in Table 2. As shown, the antisite defects are preferentially formed and vacancies are mainly formed on the Ni sublattice. Note that, the defect formation energies measured by positron lifetime spectroscopy experiments should be compared with $\tilde{E}_{\mathrm{defect}}$ rather than E_{defect}, since the former is dependent on the alloy composition while the latter is dependent on the reference states of pure elements. As shown in Table 2, our calculations are in good agreement with the experiments.

Table 1. Point defect formation energies (in units of eV) in $\mathrm{Ni_3Al}$ with and without solutes in comparison with those from the literature.

		V_{Al}	V_{Ni}	Ni_{Al}	Al_{Ni}
No solutes	This work	3.676	1.629	2.045	–1.001
	Others	3.163[a]	1.218[a]	2.011[a]	–0.854[a]
		3.57[b]	1.64[b]	1.95[b]	–0.84[b]
		2.408[c]	1.646[c]	0.832[c]	0.602[c]
Cr	M_{Ni}	3.360	1.710	1.554	–0.736
	M_{Al}	3.610	1.733	0.511	–2.370
Co	M_{Ni}	3.656	1.660	1.987	–0.965
	M_{Al}	3.536	1.622	1.911	–1.144
Mo	M_{Ni}	3.150	1.638	1.470	–0.692
	M_{Al}	3.647	1.699	0.055	–2.670
Ru	M_{Ni}	3.533	1.582	1.830	–0.972
	M_{Al}	3.531	1.660	1.125	–1.624
W	M_{Ni}	3.151	1.721	1.438	–0.607
	M_{Al}	3.643	1.738	–0.089	–2.810
Re	M_{Ni}	3.293	1.677	1.482	–0.709
	M_{Al}	3.575	1.742	0.096	–2.608
Ti	M_{Ni}	3.061	1.629	1.578	–0.660
	M_{Al}	3.716	1.636	0.340	–2.508
Nb	M_{Ni}	2.891	1.546	1.473	–0.628
	M_{Al}	3.705	1.593	–0.095	–2.780
Ta	M_{Ni}	2.965	1.645	1.461	–0.582
	M_{Al}	3.715	1.655	–0.131	–2.850

[a]Ref. [39], [b]Ref. [40], [c]Ref. [41].

Table 2. Effective formation energies (in units of eV) of point defects in stoichiometric $\mathrm{Ni_3Al}$.

	V_{Al}	V_{Ni}	Ni_{Al}	Al_{Ni}
This work	1.974	1.372	0.560	0.560
Experiments	2.01[a]	1.65[a]		
	2.180[b]	1.781[b]		
		1.6[c]		

[a]Ref. [42], [b]Ref. [43], [c]Ref. [44].

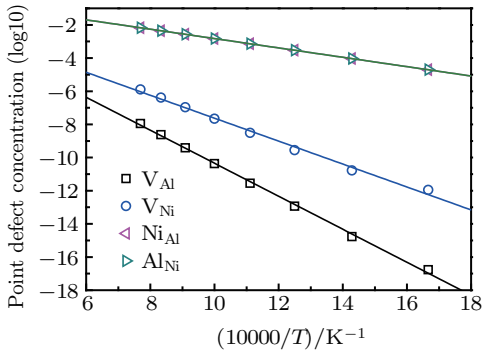


Fig. 2. (color online) Equilibrium point defect concentrations in stoichiometric $\mathrm{Ni_3Al}$ as a function of temperature.

In multi-component superalloys, a variety of alloying elements dissolve in $\mathrm{Ni_3Al}$. Therefore, the solutes can influence the formation of Ni and Al vacancies and antisite atoms in $\mathrm{Ni_3Al}$. In order to gauge the maximum effect of the solutes on the point-defect energy, the solutes were placed in the NN positions of the point defect. Table 1 summarizes the influence of ternary solutes on formation energies of point defects. For the M_{Ni}, M is predicted to decrease the defect-formation energies of $\mathrm{V_{Al}}$ and $\mathrm{Ni_{Al}}$, while increase that of $\mathrm{Al_{Ni}}$. The effect of

the solutes on the formation energy of V_{Ni} is negligible. For the M_{Al}, the effect of the solutes on the point-defect energy is similar to that of Al, except that Ti, Nb, and Ta increase the formation energy of V_{Al}.

It is known that vacancy-mediated diffusion is governed by the vacancy formation and vacancy-atom exchange process. The formation vacancy is a prerequisite for alloying element diffusion and the concentration of point defects may influene the diffusion rate.

3.2. Diffusion of solutes

In the $L1_2$ ordered Ni_3Al intermetallic compounds, certain vacancy-mediated diffusion mechanisms possibly work, such as six-jump-cycle (6JC), sublattice assisted diffusion (AS), antistructure bridge (ASB), etc.[45] The 6JC consists of six jumps and the energy barrier for the cycle is higher than the other mechanisms,[40] so the important diffusion mechanisms relevant to the diffusion behavior of Al in Ni_3Al are AS and ASB jump as shown in Fig. 3. The major component (Ni) of Ni_3Al forms a lattice structure that enables nearest neighbor (NN) jumps through the respective sublattice without producing disorder in the $L1_2$ structure. The majority component and minority component may diffuse mainly in such a Ni sublattice. As shown in Fig. 3, a Ni atom can exchange with a NN vacancy on its own sublattice as the intra-sublattice jump. However, an Al atom jumps into the "wrong" sublattice (inter-sublattice jump) that always introduces disorder in the lattice, and continues its migration through the Ni sublattice. Since the concentration of antisite defects is higher that of Ni and Al vacancies in Ni_3Al, the Al and Ni antisites play an important role in diffusion processes in $L1_2$ intermetallics, which can drastically enhance the mobility at higher temperatures.[46,47] The ASB mechanism for Al atoms consists of two jumps: (i) a vacancy and an adjacent Al atom exchange their positions, (ii) an NN anti-structure Al_{Ni} atom jumps into the new vacant position on the Al sublattice. Similarly, the ABS mechanism for Ni atoms involves the exchange of a Ni vacancy with an NN anti-structure Ni_{Al} atom, and then with a regular atom on the Ni sublattice. Two Al atoms (or Ni atoms), namely, regular sublattice and antisite, participate in the ASB jump and exchange their own lattices. As the result of accomplishing the ASB jump, the vacancy can jump up to the fourth coordination shell from its initial position, resulting in a large geometrical factor and increasing its contribution to the diffusivity. The steps of the ASB jump are presented in Fig. 3. Based on the available experimental data on the Al-substituting solute diffusion, Divinski *et al.*[12] suggested that a diffusion model of the minority component via Ni sublattice as anti-structure defects in combination with the ASB mechanism also mediates the diffusion of Al-substituting solutes.

Table 3. Various energy barriers (in units of eV) for NN, NNN, AS, and ASB sublattice jumps for Ni and Al in $L1_2$ Ni_3Al. Experimental data and previous calculations are also listed for comparison.

Jump		This work	Other calculations	Experiments
NN	$Ni_{Ni} \rightarrow V_{Ni}$	0.929	0.98[a]	1.2[e]
			1.03[b]	
			0.97[c]	
			0.696[d]	
	$Ni_{Ni} \rightarrow V_{Al}$	0.895	0.97[a]	
	$Al_{Al} \rightarrow V_{Ni}$	1.001	0.96[a]	
NNN	$Ni_{Ni} \rightarrow V_{Ni}$	3.696	3.70[a]	
	$Al_{Al} \rightarrow V_{Al}$	3.382	3.30[a]	
AS	$Al_{Ni} \rightarrow V_{Ni}$	0.723	0.80[a]	
ASB	$Al_{Al}+V_{Ni} \rightarrow Al_{Ni}+V_{Al}$	0.859	0.85[a]	
	$V_{Al}+Al_{Ni} \rightarrow V_{Ni}+Al_{Al}$			
	$Ni_{Al}+V_{Ni} \rightarrow Ni_{Ni}+V_{Al}$	0.930	0.94[a]	
	$V_{Al}+Ni_{Ni} \rightarrow V_{Ni}+Ni_{Al}$			

[a]Ref. [40], [b]Ref. [48], [c]Ref. [49], [d]Ref. [41], [e]Ref. [44].

The calculated migration energy barrier of elementary jumps for Ni and Al in Ni_3Al is listed in Table 3, which agrees well with previous calculations and available experimental values. For the NN jump, the migration energies of $Ni_{Ni} \rightarrow V_{Ni}$ and $Ni_{Ni} \rightarrow V_{Al}$ are similar, with the value of ~ 0.9 eV. However, the NNN jumps for Ni and Al atoms have higher energy barriers than the NN jumps. This may be correlated with the distance of the diffusion path, the complex neighborhood environment, and the strong interactions. It indicates that the NN jump for Ni and Al atoms is energetically favorable and Al atoms will likely diffuse with the adjacent Ni vacancies.

Figures 3(b)–3(d) show the migration energies of solutes via one-step NN jump ($M_{Al} \rightarrow V_{Ni}$), AS jump, and ASB jump. According to our previous work about the site preference of ternary alloying additions, most metal elements exhibit a strong Al site preference in the dilute ternary ordered $L1_2$ structure.[50] For the one-step NN jump, the solutes that preferentially occupy Al sites jump from the Al to the Ni sublattice, resulting in an inter-sublattice jump. From Fig. 3(b), we see that the barrier energies for all solutes are higher than that for Al, which indicates that the addition of solutes into the γ' phase contributes to the inhibition of overall mass transport. In addition, all the minimum energy pathways (MEPs) for the inter-sublattice jump are asymmetric and the maximum energy appears at the position deviating from the midpoint of each step. Unlike the γ-forming elements (Cr, Co, Mo, Ru, W, Re), γ'-forming elements (Al, Ti, Nb, Ta) reach the maximum energy at a position close to the final state (M_{Ni}, endpoint structure). These resulted from the asymmetric defect structure and local atomic environment through which the vacancy passes, as shown in Fig. 3(a). After the $M_{Al} \rightarrow V_{Ni}$ inter-sublattice jumps, solutes M and Al are located at FNN positions. Because γ'-forming elements have larger atomic radii, the atomic environment around the M–Al pairs has a lattice distortion, leading to a high energy state. As shown in Table 4, the final state wherein a solute atom occupies the Ni sublattice is

metastable and has a higher energy than the initial state where the solute occupies the Al sublattice. The energy difference between the final and initial states for Co is less than that for Al, while the energy increment for other solutes is higher than that for Al. It can be seen that Co atoms substitute at either an Al or Ni sublattice with a slight preference for the Al sublattice, whereas other solutes preferentially substitute at the Al sublattice. The above results agree with our previous reports about the site preference of transition metal elements in $L1_2$ Ni_3Al.[50]

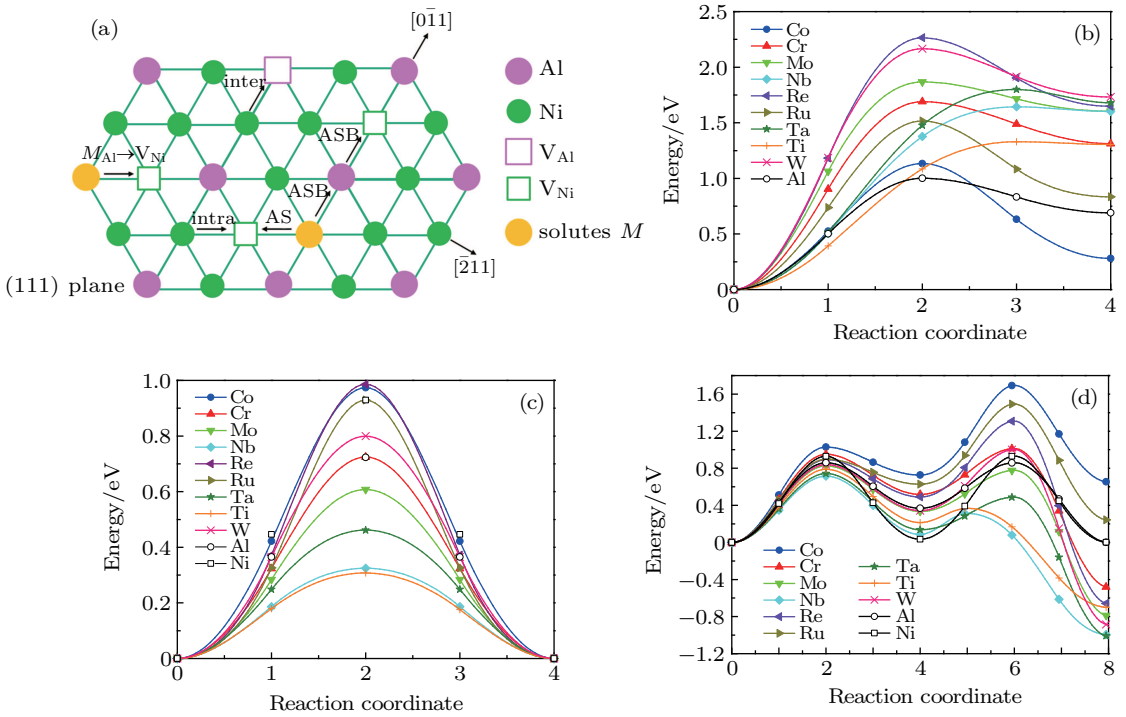


Fig. 3. (color online) Diffusion pathways and minimum energy pathways for various jump mechanisms for solutes. (a) A scheme of the intra-sublattice, inter-sublattice, AS, and ASB mechanism in $L1_2$ Ni_3Al. (b) Minimum energy pathways for M_{Al} →V_{Ni} jump. (c) Minimum energy pathways for AS jump. (d) Minimum energy pathways for ASB jump.

Table 4. Energy difference (in units of eV) between the steady and the metastable states.

Solutes	Co	Cr	Mo	Ru	W	Re	Al	Nb	Ti	Ta
This work	0.280	1.312	1.604	0.834	1.733	1.649	0.690	1.602	1.305	1.679
Others[a]	0.20	1.29					0.69		1.32	

[a]Ref. [40].

The schematics of the possible jump pathways and MEP plots for AS and ASB mechanisms for solutes diffusion in Ni_3Al are shown in Fig. 3, and the energy barriers for candidate mechanisms are listed in Table 5. For the AS mechanism, the migration energy of Re in Ni_3Al with the AS mechanism is larger than that of other elements. Interestingly, the corresponding migration energy of the alloying elements for the AS jump in the ordered γ'-Ni_3Al is less than that in the γ-Ni matrix, but the change in the energy barrier of Ni, Co, and Al is not much. For the ASB mechanism, the migration energy of Co is higher than that of other elements, these results may be related with the site preference of solutes in Ni_3Al. Similar to the diffusion behavior of alloy elements in the matrix phase, the migration energy of the γ'-forming elements (Ti, Nb, Ta) is smaller than that of the γ-forming elements (Co, Cr, Ru, W, Re) for both AS and ASB mechanisms. However, the migration energy of Mo is lower than that of Al for AS and ASB mechanisms.

Obviously, the AS mechanism has a lower energy barrier than the other candidate mechanisms for elemental (except Co) diffusion. However, the alloying element must occupy the Ni sublattice and a Ni vacancy must occupy the NN position of the solutes for this jump to occur. These restrictions will likely result in a lower jump rate of the solute atoms compared to Ni atoms because most solutes exhibit a strong Al site preference in the ordered $L1_2$ structure for multi-component superalloys. Due to Co occupying either Al or Ni sublattice in the ordered γ'-Ni_3Al, the Co atoms jump from the Ni sublattice to the Al sublattice facing the competition of anti-structure Al_{Ni} atoms. Therefore, the migration energy of Co with the AS mechanism is higher than that of other solutes. In general, the stronger the preference for the Al site, the lower the energy barrier of solutes for AS and ASB mechanisms in the γ' phase.

Table 5. Calculated migration barrier (in units of eV) for various solute jumping mechanisms and site preference $\Delta E_{\rm sub} = E^{M{\rm in}\gamma'}_{\rm subAl} - E^{M{\rm in}\gamma'}_{\rm subNi}$ in $L1_2$ Ni_3Al in units of eV.

	Co	Ru	Re	Cr	W	Mo	Ti	Ta	Nb
$M_{\rm Al} \rightarrow V_{\rm Ni}$	1.134	1.516	2.264	1.690	2.166	1.867	1.329	1.799	1.643
AS	0.974	0.929	0.986	0.725	0.800	0.608	0.308	0.462	0.325
ASB	1.694	1.493	1.309	1.013	1.003	0.826	0.789	0.743	0.716
M in γ[a]	1.114	1.432	1.706	1.268	1.328	1.151	0.526	0.779	0.654
Site preference[b]	–0.103	–0.875	–1.976	–1.553	–2.199	–2.030	–1.783	–2.263	–2.204

[a]Ref. [51], [b]Ref. [50].

As shown in Table 5, the migration energy of the ASB mechanism for solutes (except Co) is slightly higher than that of the AS mechanism, and smaller than that for $M_{\rm Al} \rightarrow V_{\rm Ni}$ jumps. If the concentration of the M anti-structure atoms is high enough at elevated temperature, the ASB mechanism will play a crucial role and promote elemental diffusion. This is in qualitative agreement with the previous experimental results that the higher Al self-diffusion and Al-like elements (Ge, Ga) diffusion with respect to the Ni self-diffusion occur at elevated temperature.[12]

According the theoretical works on the diffusion in Ni_3Al, the Ni/Al self-diffusion and the solute diffusion are determined by the following main parameters:[12,43] the Ni vacancy concentration $C_{\rm V}^{\rm Ni}$, the fractions of the Al and solute M atoms at anti-structure positions ($p_{\rm Al}$ and p_M), and the jump rates of Ni, Al, and solute atoms. Note that, both AS and ASB mechanisms are governed by the contributions of the Ni vacancy and the anti-structure defect. The latter factor p_M is probably the most important one, because the vacancy formation energy of Ni for various solutes is similar as shown in Table 1. If the formation energy of the M anti-structure atom is larger than that of the Al anti-structure atoms, the probability of the ASB jumps to occur is decreased and the solute atom diffusivity is mainly determined by the $M_{\rm Al} \rightarrow V_{\rm Ni}$ and AS jumps.

It is worth noting here that, the site preference of solutes in $L1_2$ Ni_3Al is a function of alloy composition and temperature,[52,53] and there will be a certain concentration of anti-structure atoms for solutes. Therefore, the absence of formation energy for anti-structure defects may be the reason that the activation energy of solutes obtained in the first-principles study is less than the experimental results. If the solutes occupy the Ni sublattice, the fraction of M atoms $p_M = 1$. If the solutes occupy the Al sublattice, the fraction of M atoms can be written as follows:[50,52]

$$p_M = \frac{x_{M_{\rm Al}}}{x_{M_{\rm Al}} + 3x_{M_{\rm Ni}}} = \frac{1}{1 + 3\exp\left(-\dfrac{E_{M_{\rm Ni}} - E_{M_{\rm Al}}}{k_{\rm B}T}\right)}, \quad (9)$$

where $x_{M_{\rm Al}}$ and $x_{M_{\rm Al}}$ are the concentrations of solutes on the Al and Ni sublattices, respectively. $E_{M_{\rm Al}}$ and $E_{M_{\rm Ni}}$ are the substitution formation energies of solutes on the Al and Ni sublattices, respectively, and the values are given in Table 5. According to Eq. (8), the diffusion coefficients of solutes via the AS mechanism are presented in Table 6. It can be seen that the diffusion coefficient of solutes is drastically reduced with the site preference from Ni to Al. The diffusion coefficients for Ni and Al with no solutes in stoichiometric Ni_3Al are in good agreement with the available experimental results. The experimental results for solutes are within the range between the diffusivity for occupying Al and the diffusivity for occupying Ni, indicating that the concentration of solutes on the Ni sublattice is considerable in Ni_3Al at given composition and temperature. Therefore, in addition to the migration barrier, the effect of the anti-structure defect on the diffusion of solutes is also important. Further, accurately calculating the fraction of solutes in the Ni sublattice is necessary.

Table 6. Diffusivity (in units of m^2/s) for Al, Ni, and solutes in the $L1_2$ γ'-Ni_3Al phase at 1100 °C in comparison with available experimental results.

Solute	This work		Experiments
	$M_{\rm Al}$	$M_{\rm Ni}$	
Cr	4.86×10^{-15}	1.91×10^{-20}	
Co	4.15×10^{-16}	1.75×10^{-16}	
Mo	6.83×10^{-15}	1.43×10^{-21}	3.95×10^{-17}[a]
Ru	8.63×10^{-16}	1.58×10^{-18}	
W	1.49×10^{-15}	4.26×10^{-23}	1.39×10^{-19}[b]
Re	5.31×10^{-16}	7.05×10^{-23}	
Ti	5.49×10^{-14}	1.4×10^{-19}	5.92×10^{-17}[c]
Nb	3.51×10^{-14}	3.46×10^{-21}	2.03×10^{-17}[c]
Ta	1.34×10^{-14}	6.59×10^{-22}	
Al	9.14×10^{-17}		2.82×10^{-16}[d]
Ni		6.15×10^{-16}	1.03×10^{-15}[c]

[a]Ref. [17], [b]Ref. [18], [c]Ref. [12], [d]Ref. [16].

4. Summary

By first-principles calculations with the KMC methods, the diffusion behavior of solutes via various vacancy-mediated diffusion mechanisms in $L1_2\gamma'$-Ni_3Al were investigated. For the stoichiometric Ni_3Al intermetallics, the Al_{Ni} and Ni_{Al} antisite atoms are preferentially formed. Vacancy formation on the Ni sublattice is energetically more favorable than on the Al sublattice. Adding alloying elements can decrease the defect-formation energies of Ni_{Al} and increase the defect-formation energies of Al_{Ni}. The effect of solutes on the formation energy of V_{Ni} is negligible.

The $M_{Al} \rightarrow V_{Ni}$ mechanism has a higher energy barrier than the AS and ASB mechanisms for solute (except Co) diffusion. For the $M_{Al} \rightarrow V_{Ni}$ mechanism, the barrier energies for solutes are higher than those for Al. For the AS and ASB mechanisms, the migration energy of the γ'-forming elements (Ti, Nb, Ta) is smaller than that of the γ-forming elements (Co, Cr, Ru, W, Re). The migration energy of solutes is related to the site preference of transition metal elements in $L1_2$ Ni_3Al.

To account for the available experimental data on the solute diffusion, various diffusion mechanisms for solutes contribute to the diffusivity in Ni_3Al. The concentration of antisite defects plays a crucial role in the elemental diffusion and determines which diffusion mechanism gives the predominant contribution.

Acknowledgment

The simulations were carried out on the "Explorer 100" cluster system of the Tsinghua National Laboratory for Information Science and Technology, Beijing, China.

References

[1] Reed R C 2006 *The Superalloys: Fundamentals and Applications* (New York: Cambridge University Press)
[2] Pollock T M 2016 *Nat. Mater.* **15** 809
[3] Suzuki A, Inui H and Pollock T M 2015 *Annu. Rev. Mater. Res.* **45** 345
[4] Jiang L, Li S and Han Y 2017 *IOP Conf. Ser.: Mater. Sci. Eng.* **182** 012059
[5] Liu Z and Gao W 2001 *Oxid. Met.* **55** 481
[6] Nathal M V and Ebert L J 1985 *Metall. Trans. A* **16** 1863
[7] Mishima Y, Ochiai S, Hamao N, Yodogawa M and Suzuki T 1986 *Transactions of the Japan Institute of Metals* **27** 648
[8] Kamaraj M 2003 *Sadhana* **28** 115
[9] Kovarik L, Unocic R R, Li J and Mills M J 2009 *JOM* **61** 42
[10] Eggeler Y M, Müller J, Titus M S, Suzuki A, Pollock T M and Spiecker E 2016 *Acta Mater.* **113** 335
[11] Titus M S, Mottura A, Babu Viswanathan G, Suzuki A, Mills M J and Pollock T M 2015 *Acta Mater.* **89** 423
[12] Divinski S V, Frank S, Södervall U and Herzig C 1998 *Acta Mater.* **46** 4369
[13] Cserháti C, Szabó I A, Márton Z and Erdélyi G 2002 *Intermetallics* **10** 887
[14] Shi Y, Frohberg G and Wever H 1995 *Phys. Stat. Sol. A* **152** 361
[15] Fujiwara K and Horita Z 2002 *Acta Mater.* **50** 1571
[16] Cserháti C, Paul A, Kodentsov A A, van Dal M J H and van Loo F J J 2003 *Intermetallics* **11** 291
[17] Minamino Y, Yoshida H, Jung S B, Hirao K and Yamane T 1997 *Defect and Diffusion Forum* **143-147** 257
[18] Chen C, Zhang L, Xin J, Wang Y, Du Y, Luo F, Zhang Z, Xu T and Long J 2015 *J. Alloys Compd.* **645** 259
[19] Moniruzzaman M, Fukaya H, Murata Y, Tanaka K and Inui H 2012 *Materials Transactions* **53** 2111
[20] Mabruri E, Sakurai S, Murata Y, Koyama T and Morinaga M 2008 *Materials Transactions* **49** 1441
[21] Garimella N, Ode M, Ikeda M, Murakami H and Sohn Y H 2009 *J. Phase Equilib. Diffus.* **30** 246
[22] Ikeda T, Almazouzi A, Numakura H, Koiwa M, Sprengel W and Nakajima H 1998 *Acta Mater.* **46** 5369
[23] Watanabe M, Horita Z and Nemoto M 1997 *Defect and Diffusion Forum* **143-147** 345
[24] Kresse G and Furthmüller J 1996 *Phys. Rev. B* **54** 11169
[25] Blöchl P E 1994 *Phys. Rev. B* **50** 17953
[26] Kresse G and Joubert D 1999 *Phys. Rev. B* **59** 1758
[27] Perdew J P, Burke K and Ernzerhof M 1996 *Phys. Rev. Lett.* **77** 3865
[28] Methfessel M and Paxton A T 1989 *Phys. Rev. B* **40** 3616
[29] Monkhorst H J and Pack J D 1976 *Phys. Rev. B* **13** 5188
[30] Mehrer H 2007 *Diffusion in Solids: Fundamentals, Methods, Materials, Diffusion-Controlled Process* (New York: Springer Berlin Heidelberg)
[31] Schottky W and Wagner C 1931 *Zeitschr. Phys. Chem. B* **11** 163
[32] Jiang C, Sordelet D J and Gleeson B 2006 *Acta Mater.* **54** 1147
[33] Eyring H 1935 *J. Chem. Phys.* **3** 107
[34] Vineyard G H 1957 *J. Phys. Chem. Solids* **3** 121
[35] Hänggi P, Talkner P and Borkovec M 1990 *Rev. Mod. Phys.* **62** 251
[36] Sun M, Li Z, Zhu G Z, Liu W Q, Liu S H and Wang C Y 2016 *Commun. Comput. Phys.* **20** 603
[37] Henkelman G, Uberuaga B P and Jónsson H 2000 *J. Chem. Phys.* **113** 9901
[38] Voter A F 2007 *Radiation Effects in Solids* (Dordrecht: Springer Netherlands) pp. 1–23
[39] Zhang X, Deng H, Xiao S, Tang J, Deng L and Hu W 2014 *J. Alloys Compd.* **612** 361
[40] Gopal P and Srinivasan S G 2012 *Phys. Rev. B* **86** 014112
[41] Yu S, Wang C Y, Yu T and Cai J 2007 *Physica B* **396** 138
[42] Badura-Gergen K and Schaefer H E 1997 *Phys. Rev. B* **56** 3032
[43] Numakura H, Ikeda T, M K and Almazouzi A 1998 *Philos. Mag. A* **77** 887
[44] Wang T M, Shimotomai M and Doyama M 1984 *J. Phys. F: Met. Phys.* **14** 37
[45] Gupta D 2005 *Diffusion Processes in Advanced Technological Materials* (Heidelberg: Springer Berlin Heidelberg)
[46] Kao C R and Chang Y A 1993 *Intermetallics* **1** 237
[47] Divinski S V and Larikov L N 1997 *J. Phys.: Condens. Matter* **9** 7873
[48] Chen G X, Wang D D, Zhang J M, Huo H P and Xu K W 2008 *Physica B* **403** 3538
[49] Zhang X and Wang C Y 2009 *Acta Mater.* **57** 224
[50] Liu S H, Liu C P, Liu W Q, Zhang X N, Yan P and Wang C Y 2016 *Philos. Mag.* **96** 2204
[51] Liu S, Liu C, Ge L, Zhang X, Yu T, Yan P and Wang C 2017 *Scr. Mater.* Submitted
[52] Ruban A V and Skriver H L 1997 *Phys. Rev. B* **55** 856
[53] Jiang C and Gleeson B 2006 *Scr. Mater.* **55** 433